

The study of light scalar mesons at BESII

Liao Hongbo^a

For the BES Collaboration
Institute of High Energy Physics, CAS, Beijing 100049, China

Received: 25 October 2006

Published online: 28 February 2007 – © Società Italiana di Fisica / Springer-Verlag 2007

Abstract. The production of σ and κ in J/ψ decays is presented using 58 million J/ψ events collected at BES II detector. We also report the study of the light scalar mesons $f_0(980)$, $f_0(1370)$, $f_0(1500)$ and $f_0(1710)$ etc. in J/ψ decays.

PACS. 12.39.Mk Glueball and nonstandard multi-quark/gluon states – 13.25.Gv Decays of J/ψ , Υ , and other quarkonia – 14.40.-n Mesons

1 Introduction

Since the discovery of the J/ψ at Brookhaven [1] and SLAC [2] in 1974, more than one hundred exclusive decay modes of the J/ψ have been reported. The J/ψ decays provide an excellent source of events to study light-hadron spectroscopy and search for glueballs, hybrids, and exotic states. Recently, 5.8×10^7 J/ψ events have been obtained with the upgraded Beijing Spectrometer (BES-II) [3]. Many important results on study of the light scalar mesons and the measurements of J/ψ decays are performed based on this data sample.

2 Study of scalar mesons

2.1 σ in $J/\psi \rightarrow \omega\pi^+\pi^-$

In $J/\psi \rightarrow \omega\pi^+\pi^-$, there are conspicuous $\omega f_2(1270)$ and $b_1(1235)\pi$ signals. At low $\pi\pi$ mass, a large and broad peak due to the σ is observed.

Figure 1 shows the $\pi^+\pi^-$ invariant mass distribution from $J/\psi \rightarrow \omega\pi^+\pi^-$. Partial-wave analyses have been performed on this channel using two methods and different parametrization of σ are applied [4].

Different analysis methods and different parameterizations of the σ amplitude give consistent results for the σ pole. The average pole position is determined to be $(541 \pm 39) - i(252 \pm 42)$ MeV/ c^2 .

2.2 κ in $J/\psi \rightarrow K^+K^-\pi^+\pi^-$

We find evidence for the κ in the process $J/\psi \rightarrow K^*(890)\kappa$, $\kappa \rightarrow (K\pi)_S$. We select a $K^+\pi^-$ pair in the

^a e-mail: liaohb@mail.ihep.ac.cn

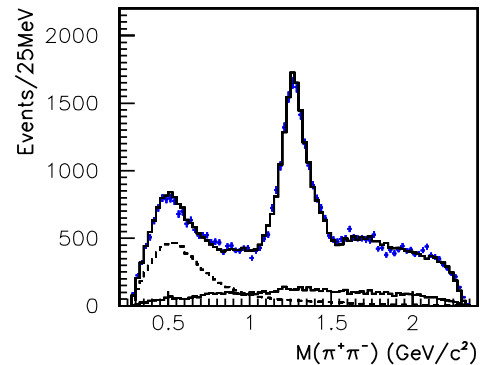


Fig. 1. The $\pi^+\pi^-$ invariant-mass distribution from $J/\psi \rightarrow \omega\pi^+\pi^-$ (crosses). The upper full histogram shows the maximum-likelihood fit, the lower full histogram corresponds to the background estimated from ω sidebands, and the dashed histogram shows the σ contribution.

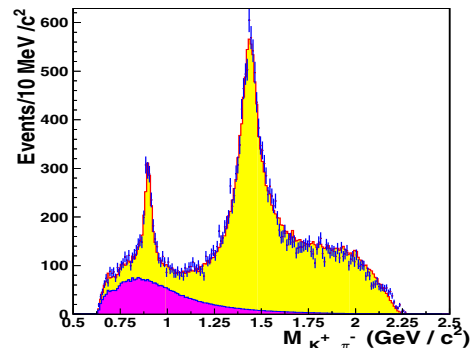


Fig. 2. $K^+\pi^-$ combinations are selected in the mass range 892 ± 100 MeV/ c^2 from $J/\psi \rightarrow K^+K^-\pi^+\pi^-$ data. The figure shows the invariant-mass distribution of accompanying $K^-\pi^+$ pairs (crosses). The upper full histogram shows the maximum-likelihood fit, the lower one shows the κ contribution.

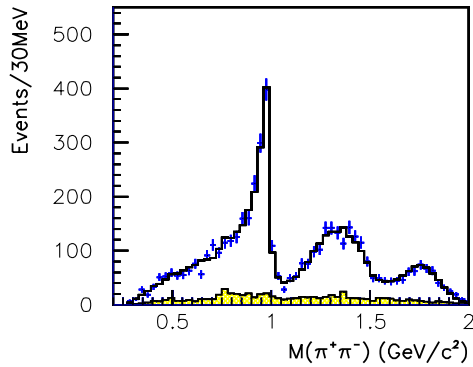


Fig. 3. The $\pi^+\pi^-$ invariant-mass distribution from $J/\psi \rightarrow \phi\pi^+\pi^-$ (crosses). The full histogram shows the maximum-likelihood fit and the shaded histogram the background estimated from ϕ sidebands.

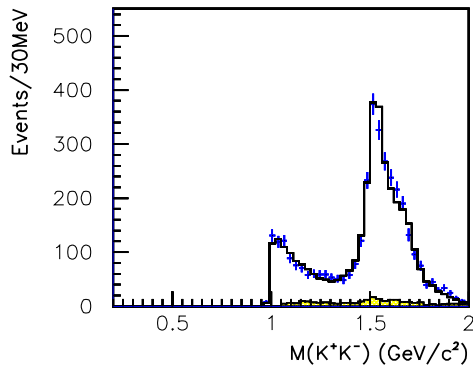


Fig. 4. The K^+K^- invariant-mass distribution from $J/\psi \rightarrow \phi K^+K^-$ (crosses). The full histogram shows the maximum-likelihood fit and the shaded histogram the background estimated from ϕ sidebands.

K^* mass range 892 ± 100 MeV/ c^2 ; fig. 2 then shows the projection of the mass of the other $K^-\pi^+$ pair.

Two independent PWA analyses have been performed. Both favor strongly the fact that the low mass enhancement of the $K^+\pi^-$ system is a resonance. The 0^+ resonances κ is highly necessary in both fits. The average values of pole position for κ is determined to be $(841 \pm 78^{+81}_{-73}) - i(309 \pm 91^{+48}_{-72})$ MeV/ c^2 [5].

2.3 Study of $J/\psi \rightarrow \phi\pi^+\pi^-$ and $J/\psi \rightarrow \phi K^+K^-$

Figures 3 and 4 show the $\pi^+\pi^-$ and K^+K^- invariant mass distribution from $J/\psi \rightarrow \phi\pi^+\pi^-$ and $J/\psi \rightarrow \phi K^+K^-$, respectively. In figs. 3 and 4, the shaded histogram corresponds to the background estimated from ϕ sidebands.

The $\phi\pi^+\pi^-$ and ϕK^+K^- data are fitted simultaneously by using partial-wave analysis [6], constraining resonance masses and widths to be the same in both sets of data. The full histogram in figs. 3 and 4 show the maximum-likelihood fit.

The $f_0(980)$ is observed clearly in both sets of data. The Flatté form

$$f = \frac{1}{M^2 - s - i(g_1\rho_{\pi\pi} + g_2\rho_{K\bar{K}})} \quad (1)$$

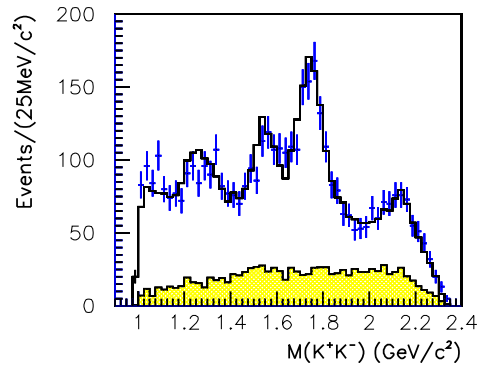


Fig. 5. The K^+K^- invariant-mass distribution from $J/\psi \rightarrow \omega K^+K^-$ (crosses). The full histogram shows the maximum-likelihood fit and the shaded histogram the background estimated from ω sidebands.

has been used to fit the $f_0(980)$ amplitude. Here ρ is the Lorentz invariant phase space, $2k/\sqrt{s}$, where k refers to π or K momentum in the rest frame of the resonance. The present data offer the opportunity to determine the parameters of $f_0(980)$ accurately: $M = 0.965 \pm 0.008(\text{stat}) \pm 0.006(\text{sys})$ GeV/ c^2 , $g_1 = 0.165 \pm 0.010(\text{stat}) \pm 0.015(\text{sys})$ GeV/ c^2 , $g_2/g_1 = 4.21 \pm 0.25(\text{stat}) \pm 0.21(\text{sys})$.

The $\phi\pi\pi$ data also exhibit a strong peak centred at $M = 1335$ MeV/ c^2 . It may be fitted with $f_2(1270)$ and a dominant 0^+ signal made from $f_0(1370)$ interfering with a smaller $f_0(1500)$ component. There is definite evidence that the $f_0(1370)$ signal is resonant, from interference with $f_2(1270)$. The mass and width of $f_0(1370)$ are determined to be: $M = 1350 \pm 50$ MeV/ c^2 and $\Gamma = 265 \pm 40$ MeV/ c^2 .

There is also a definite signal from $f_0(1790) \rightarrow \pi^+\pi^-$ with $M = 1790^{+40}_{-30}$ MeV/ c^2 , $\Gamma = 270^{+60}_{-30}$ MeV/ c^2 . It cannot arise from $f_0(1710)$, since the branching fraction ratio $K\bar{K}/\pi\pi$ for $f_0(1790)$ is a factor 14 lower than that reported in ref. [4] for $f_0(1710)$. The large discrepancy in branching fractions implies the existence of two distinct states $f_0(1790)$ and $f_0(1710)$, the $f_0(1790)$ decaying dominantly to $\pi\pi$ and the $f_0(1710)$ dominantly to $K\bar{K}$. The $f_0(1790)$ is a natural candidate for the radial excitation of $f_0(1370)$ and behaves like $f_0(1370)$.

For ϕK^+K^- data, there is a conspicuous peak due to $f_2'(1525)$, but there is a shoulder on its upper side. This shoulder is fitted mostly by $f_0(1710)$ interfering with $f_0(1500)$; there is also a possible small contribution from $f_0(1790)$ interfering with $f_0(1500)$.

2.4 Study of $J/\psi \rightarrow \omega K^+K^-$

Figure 5 shows the K^+K^- invariant-mass distribution from $J/\psi \rightarrow \omega K^+K^-$. The shaded area indicates background events from the sideband estimation. A partial-wave analysis has been performed [7], the full histogram in fig. 5 shows the maximum-likelihood fit.

A dominant feature of $J/\psi \rightarrow \omega K^+K^-$ is $f_0(1710)$, the present data are consistent with earlier studies which identify $J = 0$. The fitted $f_0(1710)$ optimises at $M = 1738 \pm 30$ MeV/ c^2 , $\Gamma = 125 \pm 20$ MeV/ c^2 .

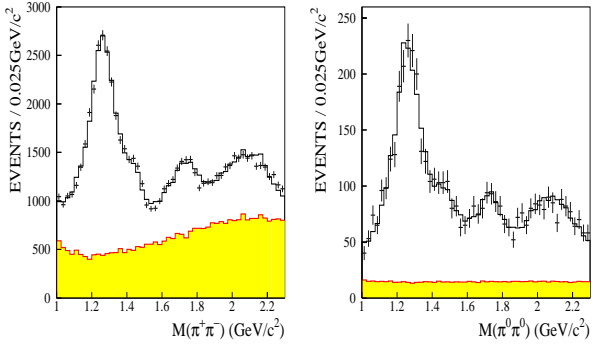


Fig. 6. Left: the $\pi^+\pi^-$ invariant-mass distribution from $J/\psi \rightarrow \gamma\pi^+\pi^-$ (crosses). The full histogram shows the maximum-likelihood fit and the shaded histogram corresponds to the $\pi^+\pi^-\pi^0$ background. Right: the $\pi^0\pi^0$ invariant-mass distribution from $J/\psi \rightarrow \gamma\pi^0\pi^0$. The crosses are data, the full histogram shows the maximum-likelihood fit, and the shaded histogram corresponds to the background.

In $J/\psi \rightarrow \omega\pi^+\pi^-$ [4], there is no definite evidence for the presence of $f_0(1710)$; if its mass is scanned, there is no optimum around $1710 \text{ MeV}/c^2$, and the fitted $f_0(1710)$ is only $0.43 \pm 0.21\%$ of $\omega\pi^+\pi^-$. In the ωK^+K^- data presented here, the $f_0(1710)$ intensity is $(38 \pm 6)\%$ of the data within the same acceptance as for $\omega\pi^+\pi^-$. The branching fraction for $J/\psi \rightarrow \omega f_0(1710)$, $f_0(1710) \rightarrow K^+K^-$ is $(6.6 \pm 1.3) \times 10^{-4}$. We find at the 95% confidence level

$$\frac{BR(f_0(1710) \rightarrow \pi\pi)}{BR(f_0(1710) \rightarrow K\bar{K})} < 0.11, \quad (2)$$

where all charge states for decay are taken into account.

2.5 Study of $J/\psi \rightarrow \gamma\pi\pi$

Figure 6 shows the $\pi^+\pi^-$ and $\pi^0\pi^0$ invariant-mass distribution from $J/\psi \rightarrow \gamma\pi^+\pi^-$ and $J/\psi \rightarrow \gamma\pi^0\pi^0$. A partial-wave analysis is carried out in the $1.0\text{--}2.3 \text{ MeV}/c^2$ $\pi\pi$ mass range [8]. There are two 0^{++} states at ~ 1.45 and $1.75 \text{ GeV}/c^2$, respectively. One 0^{++} state peaks at a mass of $1466 \pm 6 \pm 20 \text{ MeV}/c^2$ with a width of $108_{-11}^{+14} \pm 25 \text{ MeV}/c^2$, which is approximately consistent with $f_0(1500)$. However, due to the large interference between S -wave states, a possibility contribution from $f_0(1370)$ cannot be excluded. The mass and width of another 0^{++} state is $1765_{-3}^{+4} \pm 13 \text{ MeV}/c^2$ and $145 \pm 8 \pm 69 \text{ MeV}/c^2$, respectively.

A strong production of the $f_0(1710)$ signal was observed in the PWA of $J/\psi \rightarrow \gamma K\bar{K}$ [9], with a mass of $1765 \pm 4_{-25}^{+10} \text{ MeV}/c^2$ and a width of $166_{-8-10}^{+5+15} \text{ MeV}/c^2$. If the 0^{++} state at $\sim 1.75 \text{ GeV}/c^2$ observed here is interpreted as coming from $f_0(1710)$, we obtain the $\pi\pi$ to $K\bar{K}$ branching ratio as $\frac{\Gamma(f_0(1710) \rightarrow \pi\pi)}{\Gamma(f_0(1710) \rightarrow K\bar{K})} = 0.41_{-0.17}^{+0.11}$. This value is slightly higher than in $\omega\pi^+\pi^-$ and ωK^+K^- [7,10]. Hence, an alternative interpretation for this 0^{++} state is the $f_0(1790)$. This 0^{++} state may also be a superposition of $f_0(1710)$ and $f_0(1790)$.

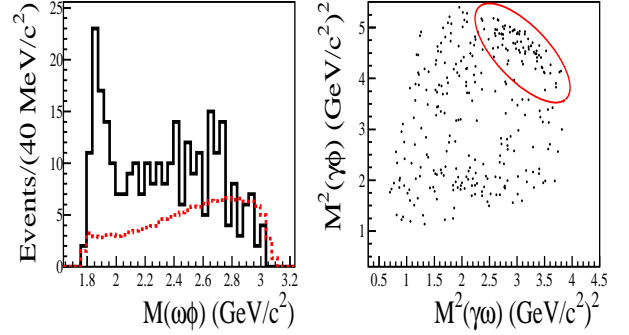


Fig. 7. Left: the $K^+K^-\pi^+\pi^-\pi^0$ invariant-mass distribution for the $J/\psi \rightarrow \gamma\omega\phi$ candidate events. The dashed curve indicates the acceptance varying with the $\omega\phi$ invariant mass. Right: Dalitz plot.

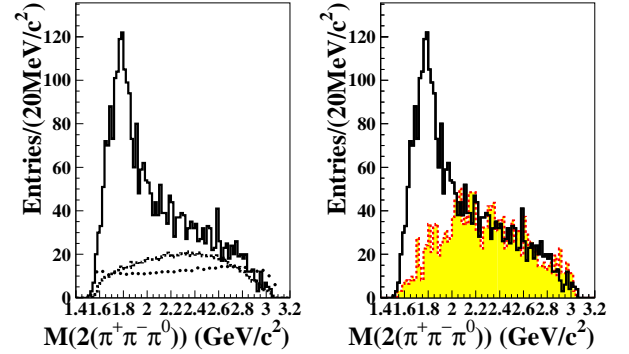


Fig. 8. Left: the $2(\pi^+\pi^-\pi^0)$ invariant-mass distribution for candidate events. The dashed curve is the phase space invariant mass distribution, and the dotted curve shows the acceptance versus the $\omega\omega$ invariant mass. Right: the $2(\pi^+\pi^-\pi^0)$ invariant mass of the inclusive Monte Carlo sample (shaded histogram).

2.6 0^{++} states in $J/\psi \rightarrow \gamma\omega\phi$ and $J/\psi \rightarrow \gamma\omega\omega$

The left panel of fig. 7 shows the $K^+K^-\pi^+\pi^-\pi^0$ invariant-mass distribution for the $J/\psi \rightarrow \gamma\omega\phi$ candidate events. The dashed curve indicates the acceptance varying with the $\omega\phi$ invariant mass. The right panel is the Dalitz plot. The detailed analysis of $J/\psi \rightarrow \gamma\omega\phi$ is described in ref. [11]. The decay modes of $\omega \rightarrow \pi^+\pi^-\pi^0$ and $\phi \rightarrow K^+K^-$ are used in the analysis.

The significance of the $\omega\phi$ threshold enhancement is more than 10σ . From a partial-wave analysis with covariant helicity coupling amplitudes, the spin-parity of the $X = 0^{++}$ with an S -wave $\omega\phi$ system is favored. The mass and width of the enhancement are determined to be $M = 1812_{-26}^{+19} (\text{stat}) \pm 18 (\text{syst}) \text{ MeV}/c^2$ and $\Gamma = 105 \pm 20 (\text{stat}) \pm 28 (\text{syst}) \text{ MeV}/c^2$, and the product branching fraction is $\mathcal{B}(J/\psi \rightarrow \gamma X) \cdot \mathcal{B}(X \rightarrow \omega\phi) = (2.61 \pm 0.27 (\text{stat}) \pm 0.65 (\text{syst})) \times 10^{-4}$. The mass and width of this state are not compatible with any known scalars listed in the Particle Data Group (PDG) [10]. It could be an unconventional state [12–16]. However, more statistics and further studies are needed to clarify this.

In the left of fig. 8, it is the $2(\pi^+\pi^-\pi^0)$ invariant-mass distribution for $J/\psi \rightarrow \gamma\omega\omega$ ($\omega \rightarrow \pi^+\pi^-\pi^0$) candidate events. The dashed curve is the phase space invariant-mass distribution, and the dotted curve shows the acceptance *versus* the $\omega\omega$ invariant mass. The right one is $2(\pi^+\pi^-\pi^0)$ invariant mass too, the shaded histogram is the inclusive Monte Carlo sample. In our analysis of $J/\psi \rightarrow \gamma\omega\omega$ [17], the presence of a signal around $1.76 \text{ GeV}/c^2$ and its pseudoscalar character are confirmed, and the mass, width, and branching fraction are measured by partial-wave analysis.

The partial-wave analysis shows that the structure around $1.76 \text{ GeV}/c^2$ in the $\omega\omega$ invariant-mass spectrum is predominantly pseudoscalar. But one 0^{++} component is needed in the fit around $1.8 \text{ GeV}/c^2$. If we use the mass and width of which was determined in $J/\psi \rightarrow \gamma\omega\phi$, the statistical significance of the 0^{++} component is 6.5σ .

3 Summary

Based on 5.8×10^7 J/ψ events accumulated at the BESII detector, the scalar mesons have been carefully studied with partial-wave analysis. The σ and κ are clearly seen in $J/\psi \rightarrow \omega\pi^+\pi^-$ and $J/\psi \rightarrow K^*K\pi, K^+K^-\pi^+\pi^-$, respectively and the corresponding pole positions are obtained. The light scalar mesons $f_0(980)$, $f_0(1370)$, $f_0(1500)$ and $f_0(1710)$ etc., have been studied in some J/ψ decay channels. The 0^{++} $\omega\phi$ threshold enhancement in $J/\psi \rightarrow \gamma\omega\phi$ is observed. And in $J/\psi \rightarrow \gamma\omega\omega$, one 0^{++} state is needed around $1.8 \text{ GeV}/c^2$ in the fit of $\omega\omega$ invariant mass spectrum.

These works of BES Collaborations are done by many people inside and outside BES Collaboration. Thank all people who contributed to these works.

References

1. J.J. Aubert *et al.*, Phys. Rev. Lett. **33**, 1404 (1974).
2. J.E. Augustin *et al.*, Phys. Rev. Lett. **33**, 1406 (1974).
3. BES Collaboration (J.Z. Bai *et al.*), Nucl. Instrum. Methods A **458**, 627 (2001).
4. BES Collaboration (M. Ablikim *et al.*), Phys. Lett. B **598**, 149 (2004).
5. BES Collaboration (M. Ablikim *et al.*), Phys. Lett. B **633**, 681 (2006).
6. BES Collaboration (M. Ablikim *et al.*), Phys. Lett. B **607**, 243 (2005).
7. BES Collaboration (M. Ablikim *et al.*), Phys. Lett. B **603**, 138 (2004).
8. BES Collaboration (M. Ablikim *et al.*), Phys. Lett. B **642**, 441 (2006).
9. BES Collaboration (J.Z. Bai *et al.*), Phys. Rev. D **68**, 052003 (2003).
10. Particle Data Group (W.-M. Yao *et al.*), J. Phys. G **33**, 1 (2006).
11. BES Collaboration (M. Ablikim *et al.*), Phys. Rev. Lett. **96**, 162002 (2006).
12. Bing An Li, hep-ph/0602072.
13. Xiao-Gang He, Xue-Qian Li *et al.*, Phys. Rev. D **73**, 051502 (2006).
14. Pedro Bicudo *et al.*, hep-ph/0602172.
15. Kuang-Ta Chao, hep-ph/0602190.
16. D.V. Bugg, hep-ph/0603018.
17. BES Collaboration (M. Ablikim *et al.*), Phys. Rev. D **73**, 112007 (2006).